# An approach to develop printable strain hardening cementitious composites

Chaves Figueiredo, Stefan; Romero Rodríguez, Claudia; Ahmed, Zeeshan Y.; Bos, D. H.; Xu, Yading; Salet, Theo M.; Çopuroğlu, Oğuzhan; Schlangen, Erik; Bos, Freek P.

**DOI**
10.1016/j.matdes.2019.107651

**Publication date**
2019

**Document Version**
Final published version

**Published in**
Materials and Design

Materials and Design 169 (2019) 107651

Contents lists available at ScienceDirect

Materials and Design

journal homepage: www.elsevier.com/locate/matdes

# An approach to develop printable strain hardening cementitious composites

Stefan Chaves Figueiredo[a,*], Claudia Romero Rodríguez[a], Zeeshan Y. Ahmed[b], D.H. Bos[b], Yading Xu[a], Theo M. Salet[b], Oğuzhan Çopuroğlu[a], Erik Schlangen[a], Freek P. Bos[b]

[a]Microlab, Faculty of Civil Engineering and Geosciences, Delft University of Technology, Delft 2628 CN, The Netherlands
[b]Department of the Built Environment, Eindhoven University of Technology, Eindhoven, The Netherlands

## HIGHLIGHTS

- A quantitative methodology based on rheological parameters to develop printable cementitious composites is presented
- The methodology was successfully applied to the development of printable strain hardening cementitious composites
- A correlation between shape stability and buildability with the initial bulk yield stress was found
- The use of VMA and the liquid/solid ratio are key factors to control mixture stability and fibre dispersion
- Rheological properties measured with the ram extruder and Benbow-Bridgwater model can suggest the build height of an object.

## GRAPHICAL ABSTRACT

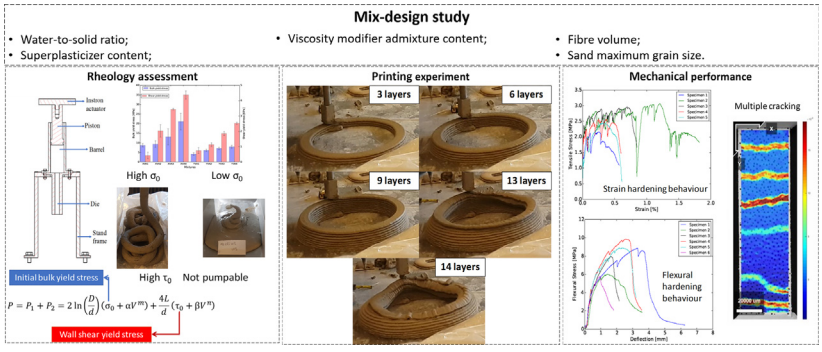


## ARTICLE INFO

*Article history:*
Received 23 October 2018
Received in revised form 8 February 2019
Accepted 9 February 2019
Available online 6 March 2019

*Keywords:*
3D printing
Rheology
Strain hardening
Additive manufacturing

## ABSTRACT

New additive manufacturing methods for cementitious materials hold a high potential to increase automation in the construction industry. However, these methods require new materials to be developed that meet performance requirements related to specific characteristics of the manufacturing process. The appropriate characterization methods of these materials are still a matter of debate. This study proposes a rheology investigation to systematically develop a printable strain hardening cementitious composite mix design. Two known mixtures were employed and the influence of several parameters, such as the water-to-solid ratio, fibre volume percentage and employment of chemical admixtures, were investigated using a ram extruder and Benbow-Bridgwater equation. Through printing trials, rheology parameters as the initial bulk and shear yield stress were correlated with variables commonly employed to assess printing quality of cementitious materials. The rheology properties measured were used to predict the number of layers a developed mixture could support. Selected mixtures had their mechanical performance assessed through four-point bending, uni-axial tensile and compressive strength tests, to confirm that strain hardening behaviour was obtained. It was concluded that the presented experimental and theoretical framework are promising tools, as the bulk yield stress seems to predict buildability, while shear yield stress may indicate a threshold for pumpability.



* Corresponding author.
*E-mail address:* S.ChavesFigueiredo@tudelft.nl (S. Chaves Figueiredo).

https://doi.org/10.1016/j.matdes.2019.107651

## 1. Introduction

Over the last decades, the employment of automation at construction sites has seen substantial achievements to enhance the productivity of the sector [1,2]. Management tools have allowed tasks and activities to become more specialized and dynamic, thus providing an environment for shortening of construction time and decreasing construction errors. The employment of machinery to execute tasks on this industry was specially devoted to heavy duties nevertheless, some other activities still rely on the skills of humans.

A relatively recent development has been the introduction of Additive Manufacturing (AM) to the construction industry, also popularly known as 3D printing. AM is a classification of manufacturing technologies that fabricate objects by controlled, often layer-wise, addition of material, rather than by removal of material from a larger piece of bulk material. Generally, robotized equipment is applied that manufacture an object directly from digital design input [3,4]. For construction, advances are being made AM of polymers [5], foams [6], glass [7], timber [8] and steel [9].

Developments have been particularly rapid for AM of concretes and other cementitious materials (AMoC) for construction. Technologies under development include the Stereolithography (STL) based D-shape process [10], Contour Crafting (CC) [11], Concrete Printing (CP) [12], 3D Concrete Printing (3DCP) [13], as well as the vertical extrusion based Smart Dynamic Casting [14] and Mesh Mould [15], in which a mesh reinforcement acts as the mould. Leaving the phase of showcasing the potential behind, described in a range of publications [16-23], AMoC (also referred to as Digitally Fabricated Concrete (DFC), to emphasize the automated production method) has now entered in a period of first real uses [24], and commercial initiatives abound (e.g. Contour Crafting, Total Kustom, WinSun, CyBe, Apis Cor, XtreeE, Incremental 3D, COBOD, and others). Alternative techniques are also available in which a mould of insulation material is printed and the concrete is cast inside [25].

This requires the development of a whole new generation of materials to meet both the manufacturing requirements (printability) as well as the mechanical and durability demands of a long-lasting. Recent researches have shown the development of cementitious composites with different aggregate particle sizes [16]. In some studies, fibres have been incorporated to stabilize the mixture at fresh state or to minimize the occurrence of cracks due to shrinkage [26].

However, as has been pointed out by other researchers as well, the different technologies and materials under development still suffer from a major drawback that forms an important obstacle for them to achieve their potential which includes form freedom, reduced material use and labour, decreased $CO_2$ emissions, and construction speed [27-31]. The print materials in AMoC, in general, have a low tensile strength compared to their compressive strength. Furthermore, they are usually brittle and thus fail relatively suddenly without large deformations. For structural use in construction, this is unacceptable, as the conventional concepts, such as the use of steel reinforcement bars, are either incompatible with AMoC or eliminate its advantages. A number of innovative approaches have been presented to overcome this problem, like the ones described by [32-34]. Further research is needed to be able to fully assess their potential and applicability.

Including fibres in the print material is an obvious solution strategy, too. It has been explored by Panda et al. [35], who compared glass fibres of different lengths (3, 6 and 8 mm) and varying volume percentage of fibres. Both studies reported a significant increase in flexural tensile strength, as well as an orientation effect of the fibres in the direction of the filament flow, but neither discussed the effects on ductility. Moreover, the use of PVA fibres in printable cementitious mortars exposed to fire attack was studied in [36]. In this case the authors have shown not only the advantages of using fibres to enhance ductility but also to minimize the occurrence of spoling. And recently the use of steel fibres to reinforce a printable mortar was also explored in [37].

Over the last decades, cementitious composites have been developed that exhibit strain hardening behaviour [38,39]. Their performance is based on an optimized matrix composition, fibre performance, and matrix-to-fibre bond, and are known as Engineered Cementitious Composites (ECCs) or Strain Hardening Cementitious Composites (SHCCs). Significant plastic deformations can be achieved, as well as a high tensile strain, strength, and multiple crack development [40]. Resistance to quasi-static and dynamic loading is generally high [41]. Jointly, this results in favourable structural performance.

First results on the development of printable ECCs have been published by Soltan & Li [42]. Based on considerations of extrudability (indicating the ability of the mixture to pass through a printing system) and buildability (indicating the ability of a mixture to remain stable after depositioning and during printing), that together define the printability, they developed several mixtures with polyvinylalcohol (PVA) fibres. The influence of several ingredients on fresh state workability and processing parameters was investigated. This resulted in at least one mixture that seems printable and shows strain hardening failure behaviour. However, the assessment of fresh state properties was based on the flow factor according to ASTM C1437 and ASTM C230, which is not a true rheological property. Also, the real printability was not truly yet established as only several layers were deposited with a manual piston. Pending a more extensive publication, a brief description of results about the development of a printable SHCC with high-density polyethylene (HDPE) fibres were given by [43].

The development of printable mix-designs is different from that of castable concretes. The challenges are not restricted to the hardened properties: competing requirements for extrudability and buildability have to be met as well. Globally speaking, the material should be fluid enough to pass through a print system without the use of excessive pressure and the occurrence of ruptures and/or void, while exhibiting sufficient strength and stiffness after depositioning to avoid failure during printing or excessive geometrical deformations. When both these requirements are met, the material can be considered printable.

In order to evaluate the printability, different tests have been proposed, such as the cylinder test [26], the slump of the fresh mixture in a shape of a cylinder [44] or the slump of the printed layer itself [45]. In general, these tests consist of measuring the slump of the fresh material with or without a certain weight on top of it. However, such empirical tests do not result in true physical properties that describe the rheological or mechanical behaviour of the material. Only recently, first attempts to analyse printability in terms of physical rheology or mechanics properties have been presented [46]. Suitable methodologies are still under development.

The requirements for materials employed in the process of manufacturing an object in AMoC through a processes like 3DCP, are similar to those for extrusion manufacturing, a process that is commonly used for several types of concrete products. Although this has been acknowledged in some reports, the mix-design often does not follow the procedure that is usually suggested in the field of extrusion research [47]. Extruded cementitious mixtures can be considered as solid suspensions. These highly concentrated suspensions usually show dough-like texture. Therefore, the employment of conventional shear-based rheometers is not always suitable. Slippage and plug-forming of the evaluated mixture may lead to unreliable results [48]. Alternatively, a ram extrusion rheometer can be used. Using the pressure measurements from this device, true rheology parameters can be determined through the Benbow-Bridgwater

**Table 1**
Chemical composition of powder raw materials.

| Compound | CEM I 42.5 N [%] | Fly ash [%] | Blast furnace slag [%] | Limestone powder [%] |
|---|---|---|---|---|
| CaO | 69.53 | 5.30 | 42.00 | 55.80 |
| $SiO_2$ | 15.6 | 53.23 | 30.73 | 0.28 |
| $Fe_2O_3$ | 3.84 | 7.77 | 0.54 | 0.03 |
| $Al_2O_3$ | 3.09 | 26.67 | 13.30 | - |
| $SO_3$ | 2.6 | 0.81 | 1.45 | - |
| MgO | 1.67 | 1.27 | 9.44 | 0.14 |
| $K_2O$ | 0.55 | 1.42 | 0.34 | - |
| $TiO_2$ | 0.31 | 1.22 | 1.01 | - |
| $P_2O_5$ | 0.14 | 0.25 | - | - |
| Rest | 0.53 | 0.52 | 0.62 | 0.03 |
| Loss on ignition | 2.14 | 1.55 | 0.57 | 43.71 |

rheology model [49-51]. A more detailed explanation of the model and the apparatus will be given in Sections 2 and 3.2.

As extrusion techniques are of great importance for the construction industry, the ram extruder proposed by Benbow-Bridgwater was extensively employed to quantify rheological parameters of different materials, amongst which a vast number of ingredients for cementitious composites. Particularly relevant to this study are reports on fibre reinforced mixtures, like the ones found in [48,52-54], with PVA fibres, or in [55,56] with natural fibres, or even with nano-fibres in [57]. The fresh state properties depend on several factors, like the volume of liquid employed, the particle size distribution, the volume of fibre reinforcement, time, and so on. Furthermore, rheology modifiers are commonly reported to have been used in studies on extruded fibre reinforced cementitious composites.

As SHCCs demonstrate enhanced mechanical performance in comparison to standard concrete or mortar, as well as superior durability properties [58,59], the systematic (i.e. based on true properties) development of printable SHCC mixtures can move AMoC forward. Therefore, this research aimed to develop a printable SHCC mix-design based on the rheology properties measured with a ram extruder and determined through the Benbow-Bridgwater model. To understand the meaning of the physical properties on the flowability, visual inspections were performed on the extruded composite. A printability trial was subsequently conducted in a large scale 3DCP facility, on selected mixtures to assess pumpability, extrudability, and buildability. After hardening, several mechanical properties were determined to show that the printable mixtures do indeed result in objects with strain-hardening failure behaviour. Only a limited number of tensile test results are shown here. The full results of the study on mechanical properties in the hardened state will be subject of a future publication.

## 2. Theoretical background

Behaving rheologically as a Bingham fluid, cementitious materials can have their yield stress measured. Measuring rheological properties of highly concentrated particle suspensions through conventional shear based rheometers has been shown as not the best approach [48,60], and alternatives were given in [49-51]. The Benbow-Bridgwater model, used commonly to study fluids such as molten plastics, clay suspensions and prefabricated cementitious material, is especially suitable for this work.

In order to evaluate the rheology of composites at the fresh state a ram extruder was employed. The ram extruder is commonly composed of an upper barrel, where the material is introduced first and a connected die land, with smaller diameter, from which the material is extruded at last. A piston, moving downwards, pushes the material from the upper barrel through the die land. Coupling the total pressure drop in the die measured with this device alongside the Benbow-Bridgwater model, a description of the fluid rheology can be obtained. The total pressure drop in the die is composed of the pressure drop of the fluid on the die entry and the pressure drop on the die land. The pressure drop does not take into consideration any pressure drop in the barrel, as it is neglectable [61]. Therefore, the total pressure drop is given by Eq. (1):

$$P = P_1 + P_2 = 2\ln\left(\frac{D}{d}\right)(\sigma_0 + \alpha V) + \frac{4L}{d}(\tau_0 + \beta V) \quad (1)$$

where:

P = Total pressure drop [kPa]
$P_1$ = Pressure drop in the die entry [kPa]
$P_2$ = Pressure drop in the die land [kPa]
$\sigma_0$ = Bulk yield stress [kPa]
$\alpha$ = Parameter characterizing speed in the die entry [kPa.s/mm]
V = Extrusion speed in the die land [mm/s]
D = Barrel diameter [mm]
d = Die diameter [mm]
$\tau_0$ = Shear yield stress [kPa]
$\beta$ = Parameter characterizing speed in the die land [kPa.s/mm]
L = Die length [mm]

For the case of extruded paste developing pseudo-plastic behaviour the influence of the extrusion speed on the total pressure drop is not linear. For such cases, the Benbow-Bridgwater model is further enriched with the coefficients m and n, as shown in Eq. (2) [61].

$$P = P_1 + P_2 = 2\ln\left(\frac{D}{d}\right)(\sigma_0 + \alpha V^m) + \frac{4L}{d}(\tau_0 + \beta V^n) \quad (2)$$

Rheological characterization of dough-like pastes is especially interesting for extruded materials, as they must keep their shape after being extruded. The resulting rheological properties are also very interesting for printed cementitious composites. Initial shear

**Table 2**
Mix design summary of X series in [$kg/m^3$].

| Mixtures nomenclature | CEM I 42.5 | Blast furnace slag | Limestone powder | PVA | VA | Superplasticizer (Glenium 51) [g] | Water |
|---|---|---|---|---|---|---|---|
| XVA1 | 265.2 | 618.9 | 884.2 | 0 | 1.8 | 17.7 | 353.7 |
| XVA2 | 264.9 | 618.0 | 882.9 | 0 | 3.6 | 17.7 | 353.2 |
| XVA3 | 264.5 | 617.2 | 881.7 | 0 | 5.2 | 17.6 | 352.7 |
| XVA4 | 264.1 | 616.3 | 880.5 | 0 | 7.0 | 17.6 | 352.2 |
| XVA3SP1 | 266.7 | 622.2 | 888.9 | 0 | 5.3 | 8.9 | 355.5 |
| XVA3SP3 | 262.4 | 612.3 | 874.7 | 0 | 5.2 | 26.2 | 349.9 |
| XVA3W1 | 224.9 | 524.7 | 749.6 | 0 | 4.5 | 15.0 | 449.7 |
| XVA3PVA10 | 261.9 | 611.0 | 872.9 | 13.0 | 5.2 | 17.5 | 349.2 |
| XVA3PVA15 | 260.6 | 608 | 868.5 | 19.5 | 5.2 | 17.4 | 347.4 |
| XVA3PVA20 | 259.2 | 604.9 | 864.1 | 26 | 5.1 | 17.3 | 345.6 |
| XVA4PVA20 | 258.9 | 604 | 862.9 | 26 | 6.9 | 17.3 | 345.2 |

**Table 3**
Mix design summary of Y series in [$kg/m^3$].

| Mixtures nomenclature | CEM I 42.5 | Fly ash | Limestone powder | Sand (125–250)$\mu$m | Sand (250–500)$\mu$m | Sand (500–1000)$\mu$m | PVA | VA | Superplasticizer (Glenium 51) [g] | water |
|---|---|---|---|---|---|---|---|---|---|---|
| YVA1 | 492.0 | 581.4 | 111.8 | 110.4 | 174.3 | 207.3 | 0 | 1.7 | 13.3 | 335.4 |
| YVA2 | 491.4 | 580.7 | 111.7 | 110.3 | 174.1 | 207 | 0 | 3.3 | 13.3 | 335.0 |
| YVA3 | 490.7 | 579.9 | 111.5 | 110.1 | 173.8 | 206.7 | 0 | 5 | 13.3 | 334.5 |
| YVA4 | 490.0 | 579.1 | 111.4 | 110.0 | 173.6 | 206.4 | 0 | 6.7 | 13.3 | 334.1 |
| YVA3SP1 | 493.7 | 583.5 | 112.2 | 110.8 | 174.9 | 208 | 0 | 5 | 6.6 | 336.6 |
| YVA3SP3 | 487.8 | 576.5 | 110.9 | 109.5 | 172.8 | 205.5 | 0 | 5 | 19.8 | 332.5 |
| YVA3W1 | 420.4 | 496.8 | 95.5 | 94.4 | 148.9 | 177.1 | 0 | 4.3 | 11.4 | 429.9 |
| YVA3PVA10 | 485.8 | 574.1 | 110.4 | 109 | 172.1 | 204.7 | 13.0 | 4.9 | 13.2 | 331.2 |
| YVA3PVA15 | 483.3 | 571.2 | 109.8 | 108.5 | 171.2 | 203.6 | 19.5 | 4.9 | 13.1 | 329.5 |
| YVA3PVA20 | 480.9 | 568.3 | 109.3 | 107.9 | 170.4 | 202.6 | 26 | 4.9 | 13.0 | 327.8 |
| YVA3PVA20-S05 | 480.9 | 568.4 | 109.3 | 186.5 | 294.4 | 0 | 26 | 4.9 | 13.0 | 327.9 |
| YVA4PVA20-S05 | 480.2 | 567.6 | 109.1 | 186.3 | 294 | 0 | 26 | 6.5 | 13.0 | 327.4 |

and bulk yield stresses are physical properties which can help in quantifying important parameters for the AM with counter craft technology. The shear yield stress quantifies the friction of the material moving through the die while the bulk yield stress is an intrinsic material property. These quantities can be related to the main mixture requirements like shape stability and printability. Moreover, these properties can also be useful to estimate the amount of layers the material is able to support.

## 3. Experimental methods

### 3.1. Materials and sample preparation

Two SHCC mixtures from [62,63] were chosen as a departure point for the development of the SHCC mixtures for 3D printing. Both mixtures were reinforced with 2% by volume of polyvinyl alcohol (PVA) fibres. The first mixture matrix was composed of ordinary Portland cement (OPC), blast furnace slag (BFS), and limestone powder (LP), while the second reported mixture is composed of OPC, fly ash (FA) and sand. In order to increase the amount of fines used in the second SHCC, additional LP was used. In Tables 2 and 3 the composition of each mixture are detailed. Initially, the rheology of their matrices (the composite without fibres) was studied. The influence of viscosity modifying agent (VA), superplasticizer (SP), water-to-solid ratio, PVA fibre volume and sand grain size on the fresh state properties was investigated.

The chemical composition of powder materials and their loss on ignition (LOI) can be found in Table 1. They were assessed by X-ray fluorescence analysis (XRF) and thermogravimetric analysis performed at 10 K/min under Argon atmosphere. The LOI was calculated using the loss of mass between 45 and 1000 °C. The particle size distribution of the raw materials can be found in Fig. 1.

VA with viscosity 201 000 mPa.s was provided by Shanghai Ying Jia Industrial Development Co., Ltd. SP used was a Glenium 51 obtained from BASF with solid concentration of 35%.

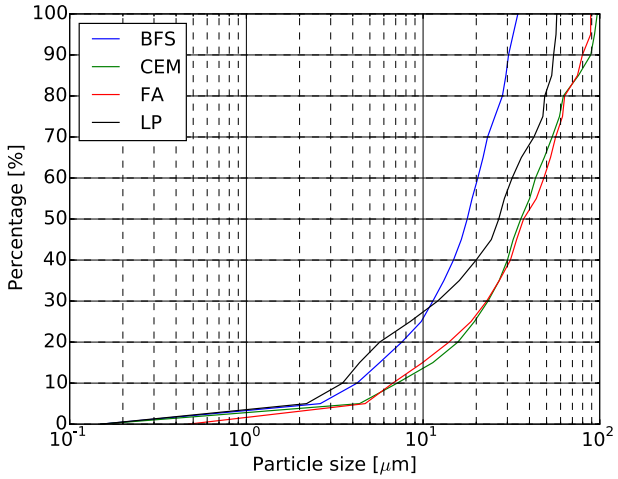


**Fig. 1.** Particle size distribution.

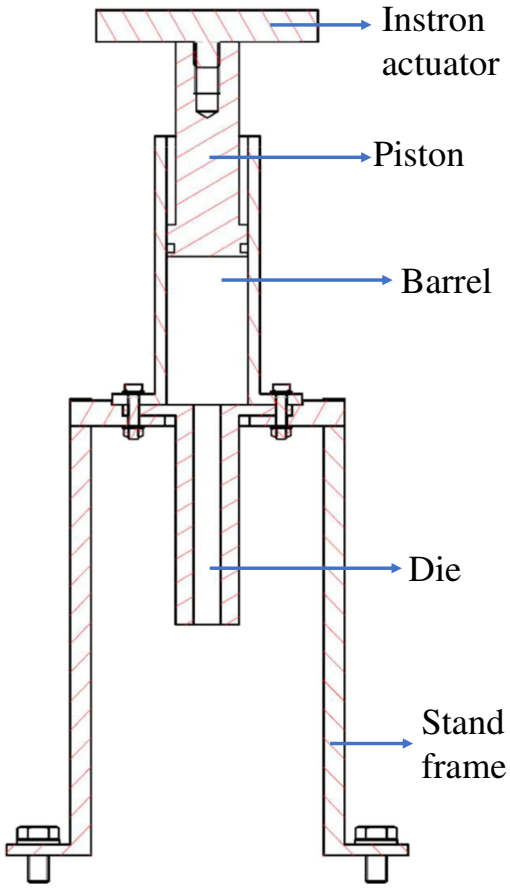


**Fig. 2.** Ram extruder and components.

For the rheology tests, a volume of 0.5 l was mixed in a planetary mixer according to the following procedure:

- All dry materials were mixed for two minutes at low speed (speed 1–60 rpm);
- While mixing at speed 1, during approximately one minute, water mixed with SP was added;
- The wet powders were mixed for the next two minutes at speed 1. In this phase it was possible to observe a significant change in the mixture's viscosity. A dough like consistence was achieved;
- At moderate speed (speed 2–124 rpm), the dough like mixture was further mixed. At this phase the dough opens inside the mixing bowl, and the fibres get dispersed.

### 3.2. Rheology measurements

In order to obtain the four parameters ($\sigma_0$, $\alpha$, $\tau_0$, $\beta$) describing the paste flow a ram extruder was built. The design was based on the equipment reported by [48,50,64] and can be found in Fig. 2. Three dies were applied with an internal diameter of 12.8 mm and length-to-diameter (L/d) ratios of 1, 4, and 8. The diameter of the piston (38.3 mm) was designed to minimize friction with the internal walls of the barrel (D = 38.4 mm) and to fit on a servo-hydraulic press (Instron 8872). Besides that, a Fluon® (polytetrafluoroethylene) ring was used as the end of the piston to seal the gap between walls and minimizing friction. During the tests this region was always lubricated with a silicone release compound (Dow Corning 7, Dow Corning®). For each new experiment the piston and the ring were removed from the Instron actuator and washed with tap water and soap.

The ram extruder barrel was filled with the mixture under evaluation. For each portion placed inside the barrel, compaction with the help of a 30 mm diameter steel rod was done. Compaction of the paste inside of the barrel is important to avoid big pockets of air which would result in drastic drop on the pressure during the extrusion experiment. As soon as the barrel was filled, the piston was attached to the Instron actuator. Four different speeds of the piston were used by controlling the displacement rate of the Instron actuator while the reaction force to the imposed displacement of the fluid was measured by a load cell. This load was used to calculate the total pressure applied to the fluid. In Fig. 3 an example of the output data

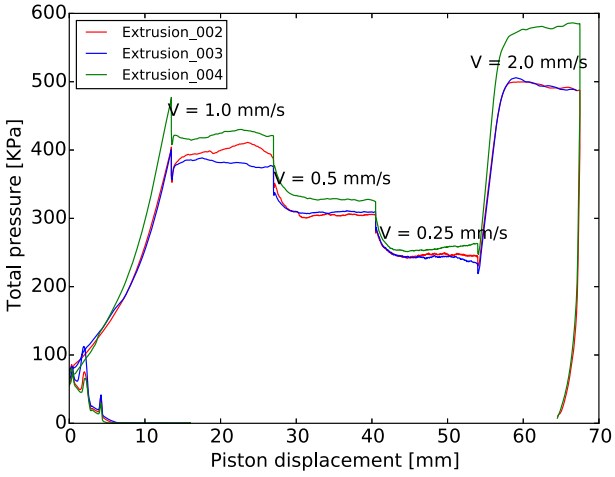


**Fig. 3.** An example of the output data from one of the rheology experiments employing the ram extruder.

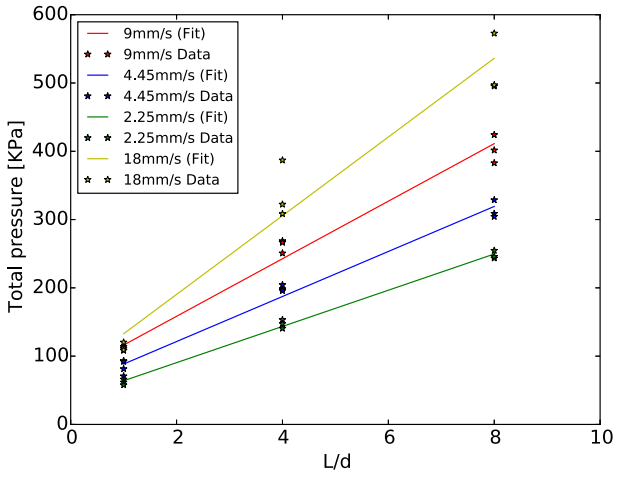


**Fig. 4.** An example of the curve fitting employing a least square method of the total pressure drop and L/d ratio.

from the experiment is given. The ram extruder experiment was performed four times for each die. The first extrusion was not considered for the test, as its only function was to aid with the appropriate filling of the die. Hence, an average of the pressure at each extrusion speed of the three repetitions was used in the calculation.

From Eq. (2) a linear relation between the total pressure applied on the fluid and L/d ratios was obtained. Curve fitting employing a least square method was used for each of the curves in order to obtain the rheology parameters that characterize the fluid. As the experiment was done for four different extrusion speeds and three L/d ratio, an average of each of the components ($\sigma_0$, $\alpha$, m, $\tau_0$, $\beta$ and n) could be obtained. Fig. 4 exemplifies the linear curve of total pressure drop versus L/d obtained from the experiment.

### 3.3. Printing trials

After the rheological characterization, printing trials were performed to assess the actual printability of the material. First, an initial test of the pumpability and extrudability was performed on 6 of the developed mixtures that were expected to show sufficient buildability based on their rheological characterization, as assessed both through visual inspection and their quantitative properties. The purpose of this trial was to establish whether the developed mixtures were compatible with the equipment, particularly whether the fibres

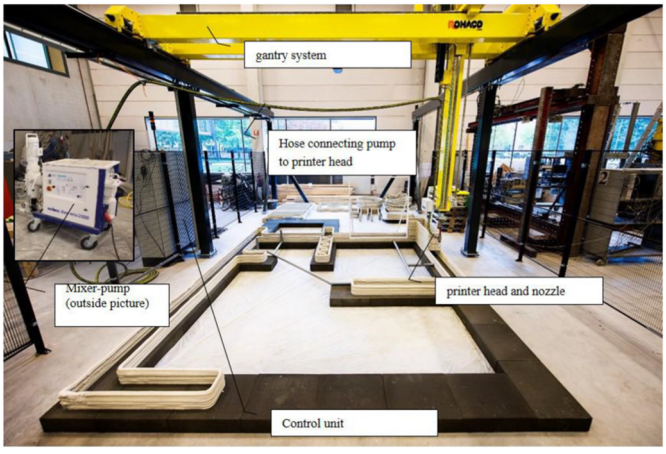


**Fig. 5.** 3D Concrete Printing facility of the Eindhoven University of Technology (TU/e) (taken from: [16]).

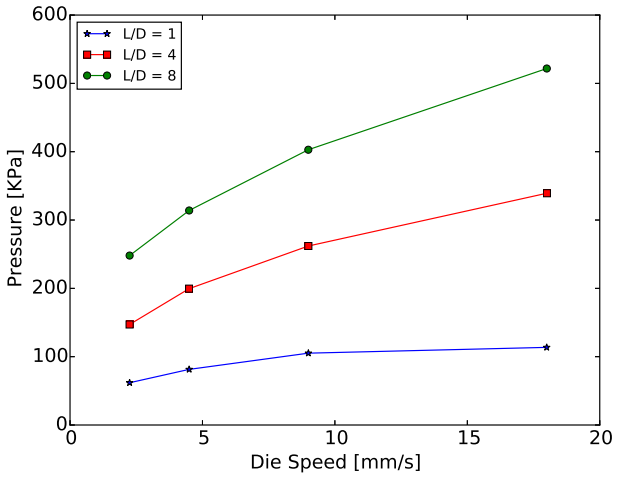


**Fig. 6.** An example total pressure on the fluid measured for different extrudate velocities.

would not cause blockage in the linear displacement pump, which features narrow cavities. Based on the observations in this initial trial, one mixture was subsequently selected for an object printing experiment.

For the preceding initial trials, mixed batches of the selected mixtures were fed to the pumping unit of the mixer-pump that is part of the 3DCP print facility of the Eindhoven University of Technology (TU/e) as described by [16]. The mixer unit of the mixer-pump was bypassed as the extent of mixing provided by this unit is insufficient for the developed mixtures. Therefore, batches were mixed using the procedure that was also applied for the rheological tests, and material from the mixed batch was inserted into the pumping unit of the mixer pump. The pump was connected to a 5 m, ø 2.5 cm hose. It was observed whether the material would be pumped without clogging, and whether the material could be transported through the hose.

In the object printing experiment, the TU/e 3DCP print facility, shown in Fig. 5, was used in its entirety (except, again, for the mixing unit of the mixer-pump). The mixer-pump was connected to the print head with the standard 10 m, ø 2.5 cm hose. The standard print nozzle with a 40 × 10 mm mouth opening was used. Cylinder shapes with a print path (heart line) diameter of 500 mm were printed until failure. The appropriate print speed was established as 5000 mm/min (or 83.3 mm/s). The print time of a single layer, thus, was approximately 0.31 min (or 19 s). This geometry has been used previously by [65] to study buildability of another mixture. Overall behaviour was visually recorded and the number of stacked layers before failure counted.

### 3.4. Mechanical tests

The composites reinforced with 2% by volume of PVA fibres were also evaluated mechanically, to verify whether strain hardening failure behaviour had indeed been obtained. For these cases, a volume of 3 l was mixed following the same procedure described earlier. Four-point bending, and compressive tests were performed to evaluate the performance of the composite. Motivated by the outcomes of the research at the rheology measurement stage, only YVA4PVA20-S05 and XVA3PVA20 mixtures were chosen to have their tensile behaviour tested.

The samples were cast and kept sealed in their moulds for three days. Afterwards, they were demoulded and cured in a curing room at (20 ± 2) °C and relative humidity of (98 ± 2)%. The compressive strength was measured at 14 and 28 days on 35 mm cubes, sawn from 40×40×160 mm beams. The samples for four-point bending test were sawn from 180×180×10 mm slabs, with approximate dimensions of 180×40×10 mm and tested at 28 days of curing. Finally, the samples for direct tensile test were sawed from 240×60×10 mm slabs, in the end reaching final dimensions of 150×40×10 mm and tested at 35 days of curing. The compressive test was done at loading rate of 2 kN/s. The four-point bending, with a test spam of 12 mm, and tensile tests were performed on the same servo-hydraulic Instron 8872 machine in which the extrusion tests were done. The employed deflection rate for the four-point bending was 0.01 mm/s and the tensile elongation rate was 1 $\mu$m/s, controlled by linear variable differential transformer (LVDT) sensors. It is important to observe that the specimens tested on uni-axial tensile test had

**Table 4**
Summary with all measured rheology parameters.

| Mixtures | $\alpha$ [kPa.s/mm] | $\beta$ [kPa.s/mm] | $\sigma_0$ [kPa] | $\tau_0$ [kPa] | m | n |
|---|---|---|---|---|---|---|
| XVA1 | 0.88 ± 0.09 | 0.14 ± 0.02 | 8.74 ± 0.90 | 0.42 ± 0.21 | 0.26 ± 0.02 | 0.24 ± 0.09 |
| XVA2 | 0.93 ± 0.17 | 0.39 ± 0.10 | 9.33 ± 1.66 | 2.03 ± 0.41 | 0.28 ± 0.04 | 0.69 ± 0.05 |
| XVA3 | 1.30 ± 0.42 | 0.69 ± 0.01 | 13.06 ± 4.18 | 3.44 ± 0.06 | 0.35 ± 0.08 | 0.81 ± 0.01 |
| XVA4 | 2.10 ± 0.44 | 0.87 ± 0.05 | 21.07 ± 4.38 | 4.36 ± 0.27 | 0.49 ± 0.08 | 0.92 ± 0.03 |
| XVA3SP1 | 2.43 ± 0.41 | 0.94 ± 0.06 | 24.11 ± 4.28 | 4.68 ± 0.30 | 0.55 ± 0.07 | 0.96 ± 0.04 |
| XVA3SP3 | 0.20 ± 0.12 | 0.75 ± 0.04 | 1.99 ± 1.21 | 3.74 ± 0.18 | 0.12 ± 0.03 | 0.85 ± 0.02 |
| XVA3W1 | 0.78 ± 0.03 | 0.15 ± 0.01 | 7.77 ± 0.26 | 0.50 ± 0.12 | 0.24 ± 0.01 | 0.28 ± 0.05 |
| XVA3PVA10 | 3.09 ± 0.54 | 0.42 ± 0.10 | 30.90 ± 5.42 | 2.07 ± 0.48 | 0.68 ± 0.09 | 0.63 ± 0.06 |
| XVA3PVA15 | 3.23 ± 0.58 | 0.46 ± 0.11 | 32.25 ± 5.76 | 2.32 ± 0.56 | 0.70 ± 0.10 | 0.66 ± 0.07 |
| XVA3PVA20 | 3.45 ± 0.51 | 0.51 ± 0.10 | 34.52 ± 5.06 | 2.53 ± 0.52 | 0.74 ± 0.08 | 0.69 ± 0.06 |
| XVA4PVA20 | 3.93 ± 0.80 | 0.97 ± 0.05 | 39.03 ± 8.31 | 4.87 ± 0.26 | 0.81 ± 0.14 | 0.98 ± 0.03 |
| YVA1 | 0.41 ± 0.07 | 0.18 ± 0.02 | 4.08 ± 0.72 | 0.74 ± 0.20 | 0.17 ± 0.02 | 0.37 ± 0.09 |
| YVA2 | 0.61 ± 0.05 | 0.23 ± 0.02 | 6.04 ± 0.54 | 1.13 ± 0.12 | 0.21 ± 0.01 | 0.51 ± 0.07 |
| YVA3 | 0.70 ± 0.06 | 0.34 ± 0.05 | 7.03 ± 0.63 | 1.85 ± 0.12 | 0.23 ± 0.01 | 0.71 ± 0.10 |
| YVA4 | 0.79 ± 0.08 | 0.50 ± 0.01 | 7.92 ± 0.83 | 2.52 ± 0.07 | 0.25 ± 0.02 | 0.70 ± 0.01 |
| YVA3SP1 | 1.33 ± 0.10 | 0.23 ± 0.01 | 13.26 ± 1.02 | 1.25 ± 0.06 | 0.36 ± 0.02 | 0.59 ± 0.04 |
| YVA3SP3 | 0.82 ± 0.06 | 0.21 ± 0.02 | 8.17 ± 0.63 | 0.99 ± 0.19 | 0.25 ± 0.01 | 0.47 ± 0.08 |
| YVA3W1 | 0.70 ± 0.07 | 0.100 ± 0.001 | 6.88 ± 0.73 | 0.102 ± 0.004 | 0.23 ± 0.01 | 0.101 ± 0.002 |
| YVA3PVA10 | 1.65 ± 0.15 | 0.28 ± 0.03 | 16.46 ± 1.47 | 1.40 ± 0.15 | 0.43 ± 0.03 | 0.56 ± 0.01 |
| YVA3PVA15 | 2.09 ± 0.23 | 0.32 ± 0.03 | 20.88 ± 2.28 | 1.59 ± 0.14 | 0.51 ± 0.04 | 0.57 ± 0.02 |
| YVA3PVA20 | 2.92 ± 0.18 | 0.19 ± 0.03 | 29.22 ± 1.83 | 0.90 ± 0.18 | 0.65 ± 0.03 | 0.46 ± 0.04 |
| YVA4PVA20 | 3.60 ± 0.19 | 0.50 ± 0.02 | 35.96 ± 1.90 | 2.51 ± 0.08 | 0.77 ± 0.03 | 0.69 ± 0.01 |
| YVA3PVA20S05 | 2.56 ± 0.19 | 0.43 ± 0.02 | 25.63 ± 1.89 | 2.16 ± 0.09 | 0.59 ± 0.03 | 0.65 ± 0.01 |
| YVA4PVA20S05 | 3.43 ± 0.20 | 0.50 ± 0.02 | 34.26 ± 1.98 | 2.49 ± 0.08 | 0.74 ± 0.03 | 0.69 ± 0.01 |

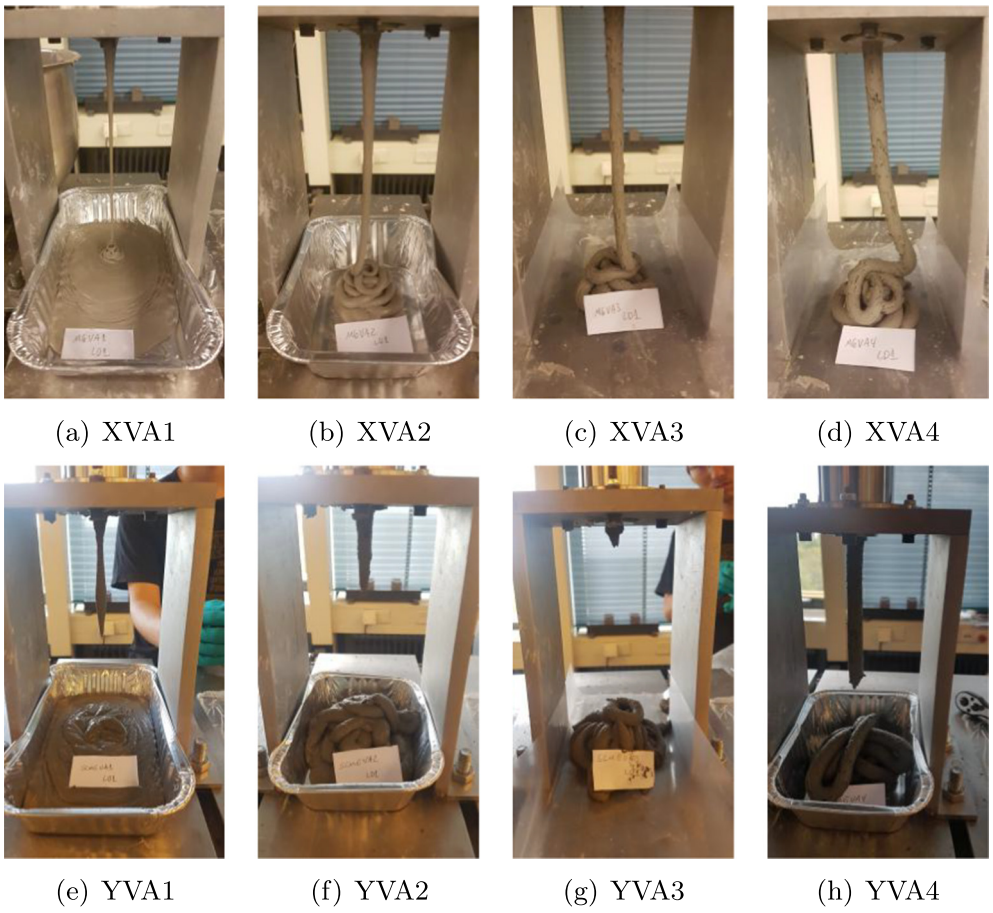


**Fig. 7.** Visual inspection of extruded material with different amounts of VA.

upper and lower side glued on steel plates. The lower side was glued inside the servo-hydraulic machine to avoid bending while testing.

Due to the high viscosity of the mixtures obtaining a homogeneous thickness while casting the samples was difficult, especially for the four-point bending specimens. Therefore, prior to the mechanical tests each individual specimen was measured at several locations.

Specimens undergoing tensile test had their frontal surface prepared for employment of digital image correlation (DIC). Their surface was painted white and randomly distributed black dots were

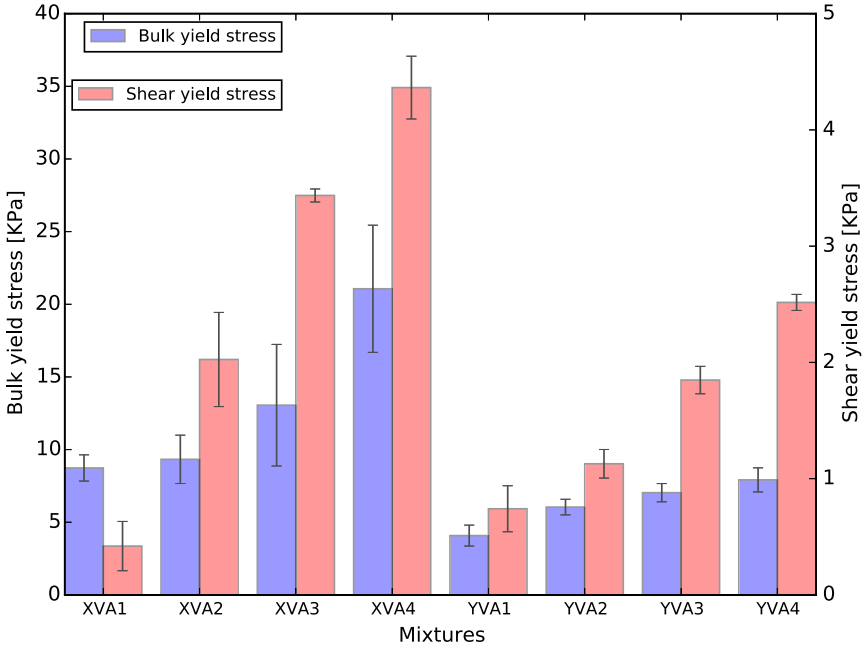


**Fig. 8.** A summary of the effect of VA content on initial bulk and shear yield stress.

(a) XVA3 (b) XVA3W1 (c) YVA3 (d) YVA3W1

**Fig. 9.** Visual inspection of extruded material for different water-to-solid ratio.

made with a permanent marker. This pattern helps in enhancing the contrast needed for the DIC software to calculate the displacements during test. The open source software Ncorr2 was employed for the DIC [66]. A Cannon camera model EOS 6D with Tamron aspherical 28–75 mm lens was employed to obtain one picture each two seconds of test. An approximate resolution of 48$\mu$m/pixel was obtained.

## 4. Results

### 4.1. Rheology

The six parameters-approach according to Eq. (2) was chosen to characterize all mixtures, as a non-linear behaviour was identified. Fig. 6 illustrates the increase of total pressure of different extrusion speeds. In the following subsections, the influence of each of the mixture variables (viscosity modifier agent, water content, superplasticizer, and fibres) is detailed. A summary of all results is shown in Table 4.

#### 4.1.1. Effect of VA content

The effect of VA was investigated on matrix level. Four dosages of methylcellulose were employed: 0.1, 0.2, 0.3 and 0.4% of the total solids weight. The water-to-solid ratio and superplasticizer added were kept constant at 0.2 and 2% by total powder weight, respectively.

For both matrices, the increase of VA content directly influenced the initial bulk and shear yield stresses, as is visually shown in Fig. 7, and quantitatively compared in Fig. 8. The increase in these rheological parameters has direct effect on the shape stability of the printed material. Therefore, the employment of VA can contribute positively to the development of printable mix designs. Greater rheological parameters values were obtained for the X matrix, indicating that solid suspensions with smaller liquid-to-particles surface area ratio are more vulnerable to changes in the viscosity of the liquid phase.

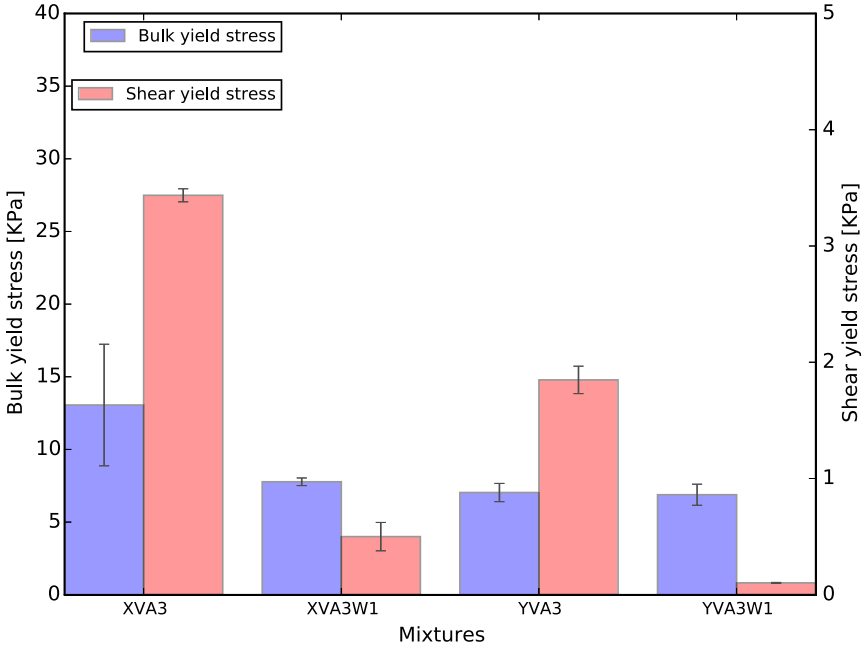


**Fig. 10.** A summary of the effect of water-to-solid ratio on initial bulk and shear yield stress.


**Fig. 11.** Visual inspection of extruded material for different SP concentrations.

This result is important to show how sensitive highly concentrated solid solutions, like the ones obtained for SHCCs or macro defect free cementitious composites, are to the adjustment of VA content.

*4.1.2. Effect of water content*

The influence of extra water in the mixtures was investigated at matrix level. By keeping the superplasticizer and methylcellulose

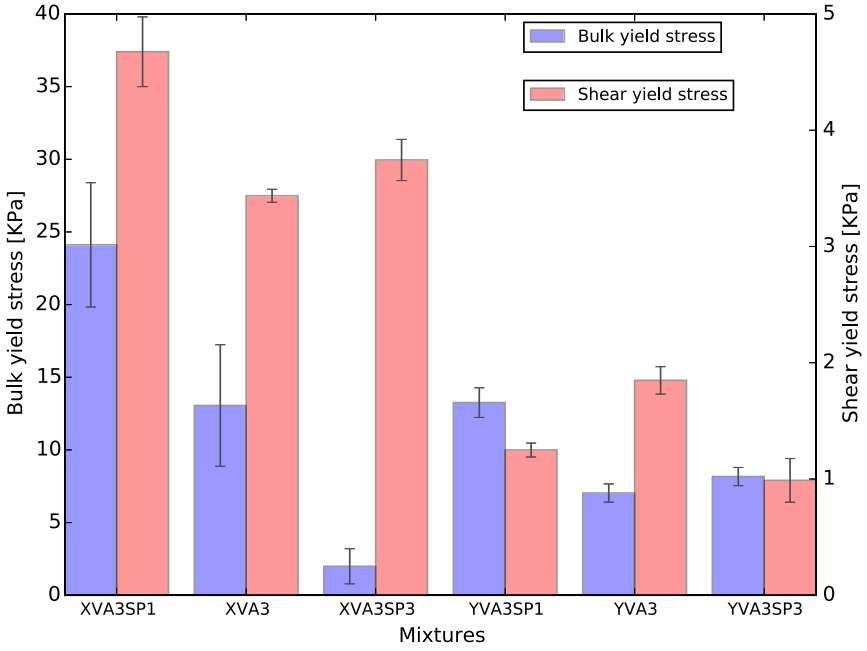


**Fig. 12.** A summary of the effect of SP content on initial bulk and shear yield stress.


**Fig. 13.** Visual inspection of extruded material for different levels of PVA fibre reinforcement.

constant, the effect of increasing the water-to-solid ratio from 0.2 to 0.3 was investigated.

As expected, a higher volume of water in the solution changes significantly the flowability of mixtures where the amount of liquid to wet the surfaces of the particles is already limited. Therefore, the decrease of X series' bulk yield stress was considerably larger than the one observed for SMCE, as reported in Fig. 10. Anyhow, as the amount of liquid to lubricate the movement of the particles against

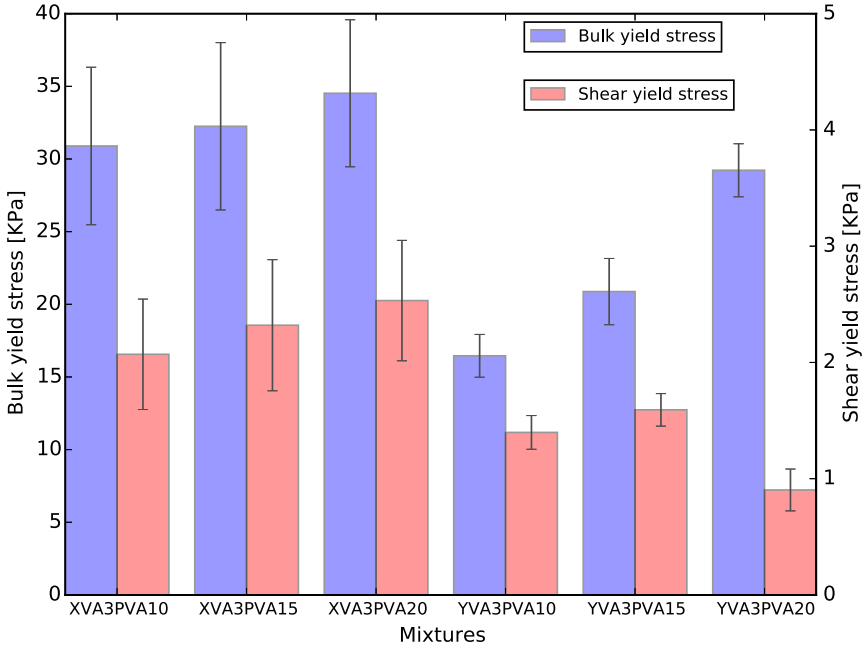


**Fig. 14.** A summary of the effect of PVA fibres volume on initial bulk and shear yield stress.


(a) YVA3PVA20 (b) YVA4PVA20 (c) YVA3PVA20S05 (d) YVA4PVA20S05

**Fig. 15.** Visual inspection of extruded material for sand maximum grain size of 0.5 mm and 1 mm.

each other is higher, the largest influence of the increase of the amount of water on the mixture can be observed on the shear yield stress. The influence of the water-to-solid ratio on the paste fluidity can be observed in Fig. 9.

*4.1.3. Effect of superplasticizer content*

A subsequent investigation targeted the effect of the superplasticizer dosage at 1, 2, and 3% of the total powder phase. Keeping constant the percentages of methylcellulose and water-to-solid ratio it could be noticed that the influence on the rheology properties was not as remarkable as the one measured when the water-to-solid ratio was investigated.

The initial bulk yield stress increased or decreased whenever the amount of superplasticizer was changed from 1 to 3% (Fig. 12). However, a decrease of approximately 32% of the initial shear yield stress when 1% of superplasticizer was employed on Y matrix was measured. This decrease might be correlated with the excess of liquid present in this solid suspension, as the particle size went up to 1 mm and there is a considerable high usage of fly ash. Visually, the influence of the amount of superplasticizer can be observed in Fig. 11.

*4.1.4. Effect of PVA fibre reinforcement*

As described in the introduction, the goal of this research was to develop a printable SHCC mix design. Therefore, the influence of 1.0, 1.5 and 2.0% by total volume of fibre reinforcement on the above described matrices was studied. For both matrices (X and Y) the content of superplasticizer, methylcellulose and water-to-solid ratio were chosen to be 2%, 0.3% and 0.2 respectively.

For both mixtures, the fibre reinforcement increased considerably the initial bulk and shear yield stresses. The values of $\sigma_0$ at least doubled when the fibre reinforcement was incorporated, as can be seen in Fig. 14. Zhou et al. 2005, explained this behaviour by attributing this increase to the raise of friction between fibres and particles in the matrix while the mixture is being extruded.

However, when the rheological properties of both mixtures were observed with the increasing volume of fibres, they demonstrated a different behaviour. The increased volume of fibres did not significantly change $\sigma_0$ and $\tau_0$ for the X composites. On the other hand, the enlarged volume of reinforcement in the Y matrix significantly increased $\sigma_0$. These dissimilar effects can be attributed to the different particle size distributions of the respective composites. The

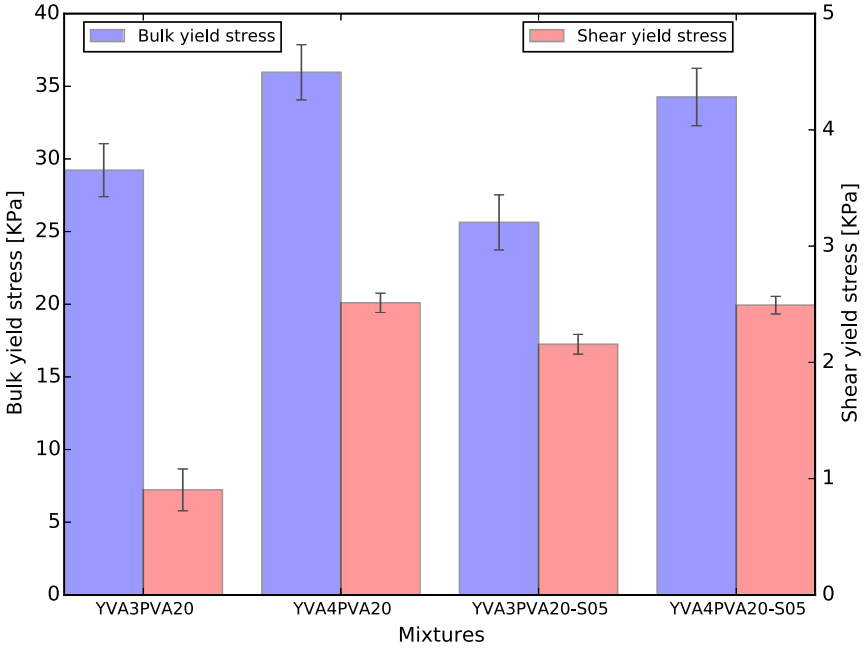


**Fig. 16.** A summary of the effect on PVA fibres volume.

**Table 5**
Results of initial pumpability and extrudability trials.

| Mixture | $\sigma_0$ [kPa] | $\tau_0$ [kPa] | Mixture can pass through... | |
|---|---|---|---|---|
| | | | Pump | 5 m hose |
| XVA3PVA20 | 34.74 ± 5.20 | 4.41 ± 0.18 | ✓ | ✓ |
| XVA4PVA20 | 39.03 ± 8.31 | 4.87 ± 0.26 | ✓ | × |
| YVA3PVA20 | 29.22 ± 1.83 | 0.90 ± 0.18 | × | (n/a) |
| YVA4PVA20 | 35.96 ± 1.90 | 2.51 ± 0.08 | × | (n/a) |
| YVA3PVA20S05 | 25.63 ± 1.89 | 2.16 ± 0.09 | ✓ | ✓ |
| YVA4PVA20S05 | 34.26 ± 1.98 | 2.49 ± 0.08 | ✓ | ✓ |

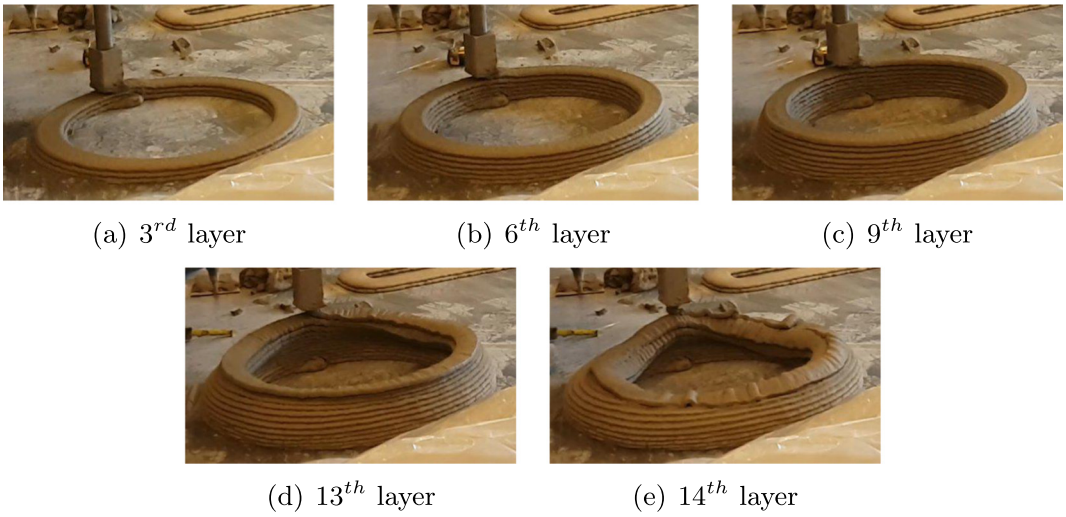


**Fig. 17.** Cylinder printing test.

X matrix was tailored to minimize the space between all the composing matrix particles, including the fibres. The Y matrix, on the other hand, presents larger gaps between the aggregates, where the increasing volume of fibres can be allocated. Visual inspections can be done with the help of Fig. 13. There the shape stability of the extruded filaments as well as the influence of the volume of fibre reinforcement and 0.4% of VA can be assessed. Comparing the rheological results obtained and summarized in Fig. 14 with the images in Fig. 13, provides a clear correlation between the shape stability and the increase values of initial bulk yield stress.

*4.1.5. Effect of sand maximum grain size on Y reinforced by 2% of PVA fibres*

Although the TU/e 3DCP facility [32] is capable of processing mixtures with a particle size of up to 2 mm, it was observed in preliminary trials that the probability of blockage in the pump system significantly decreased when a less viscous mixture was used or the maximum grain size was reduced. However, during the trials only with the pump, the probability of blockage was considerably higher when aggregates up to 1 mm were employed. This risk was only decreased when a less viscous mixture was employed at the expense of worsening the shape stability. As reported above, if more water or superplasticizer is added to this mixture the consequences would be the decrease on the initial bulk and shear yield stresses. Hence, those changes would lead to losses on the shape stability culminating with a less stable mixture which could segregate while the composite is pumped.

Therefore, the influence of the maximum grain size of sand used on Y composites was evaluated through the rheological parameters. Mixtures employing 0.3 and 0.4 wt.% of the total solid content of VA, with the maximum sand grain size of 0.5 mm, and keeping 2% of PVA fibres by volume, 2% of superplasticizer by total solid weight and 0.2 water-to-solid ratio were evaluated.

The results showed that by decreasing the maximum grain size of the sand slightly lowered the bulk yield stress of composites with 0.3 wt.% of VA, as it can be seen in Fig. 16. However, when employing 0.4 wt.% of VA, the values of $\sigma_0$ remained in the same range as the ones observed for composites employing 1 mm sand. Furthermore, the $\tau_0$ of composites with 0.3% of VA increased considerably in comparison with composites with 1 mm sand. This result demonstrates that the use of smaller maximum grain size for sand contributes to

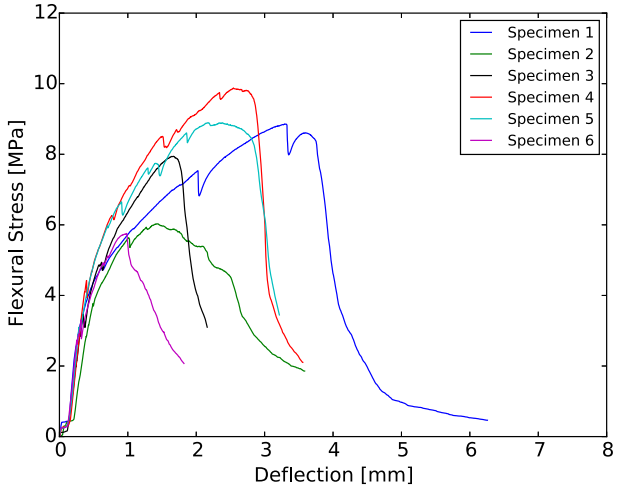


**Fig. 18.** An example from the obtained flexural hardening behaviour obtained from mixture XVA3PVA20.

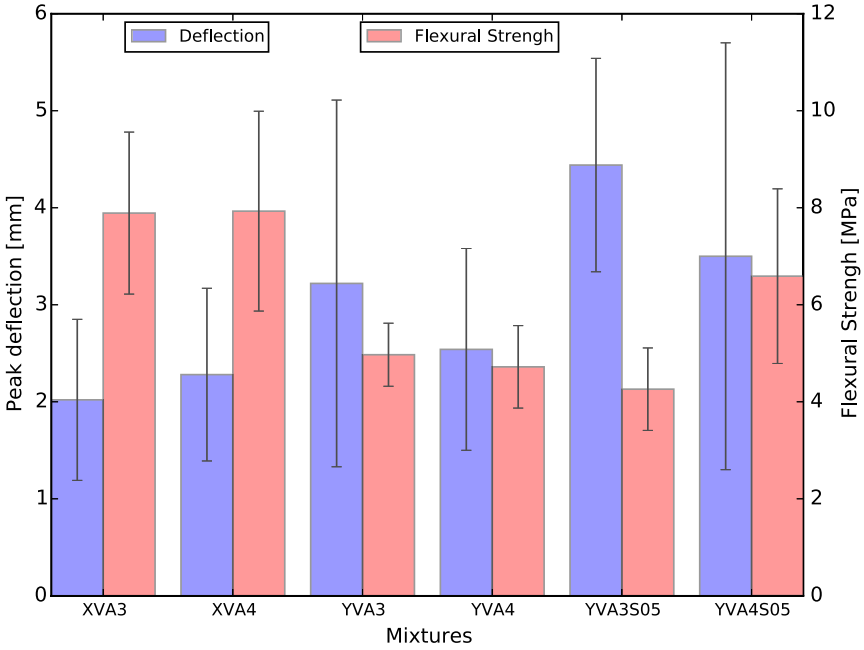


**Fig. 19.** Average performance on four point bending test of selected mixtures.

the development of a more packed composite with an initial bulk yield stress comparable to what was obtained for the X mixtures. In Fig. 15, the influence of the sand grain size and the amount of VA can be observed.

### 4.2. Printing experiments

#### 4.2.1. Initial trial

Based on the visual assessment and quantitative rheology properties, six mixtures were selected for the initial trial with the pump and a 5 m hose. The results are summarized in Table 5. Two mixtures could not be pumped as they led to blockage of the linear displacement pump. It could therefore not be established whether they could be extruded through the 5 m hose. The blockages were likely caused by the maximum grain size of the respective mixtures that turned out to be incompatible with the pumping system. Excessive bulk and shear yield stresses of these mixtures were not the cause, as they were in the same range as those of the other mixtures.

One other (XVA4PVA20) could pass through the pump, but generated too much friction in the hose to be transported through it. This seems to correspond to a limit of shear yield stress having been exceeded for the system to which the mixture was applied, as it is higher than that of three mixtures that could both be pumped and transported. Further experiments are required to further elucidate the apparent relations between the rheological parameters bulk and shear yield stress on the one hand, and mixture behaviour in the printing process.

Considering these results, for printing, the mixture with the highest bulk yield stress that still fulfils the pumpability and extrudability requirement (i.e. does not exceed the shear yield stress limit), should be selected, as it should result in optimal buildability. Thus, two mixtures (XVA3PVA20 and YVA4PVA20-S05) seem to be comparably suitable. Their shape stability is also visually apparent from the rheology tests, as shown in Figs. 13 (c) and 15(d). For practical purposes, the YVA4PVA20-S05 mixture was selected for the object printing experiment. The third mixture (YVA3PVA20-S05), while being pumpable, was expected to have lower buildability due to the lower bulk yield stress, and was thus disregarded.

#### 4.2.2. Object printing experiment

Analysis methods to predict the buildability are still under development. Wolfs et al. [65] have presented a solid mechanics based approach considering both stability and material failure effects,

**Table 6**
Compressive strength performance [MPa].

| Mix design | Load perpendicular to the casting direction | Load parallel to the casting direction |
|---|---|---|
| **XVA3** | 41.12 ± 4.18 | 41.71 ± 3.21 |
| **XVA4** | 38.26 ± 5.48 | 37.76 ± 3.45 |
| **YVA3** | 15.89 ± 0.95 | 14.37 ± 1.81 |
| **YVA4** | 14.49 ± 1.48 | 14.78 ± 1.3 |
| **YVA3S05** | 8.39 ± 1.82 | 8.49 ± 0.5 |
| **YVA4S05** | 15.47 ± 0.65 | 15.84 ± 1.58 |

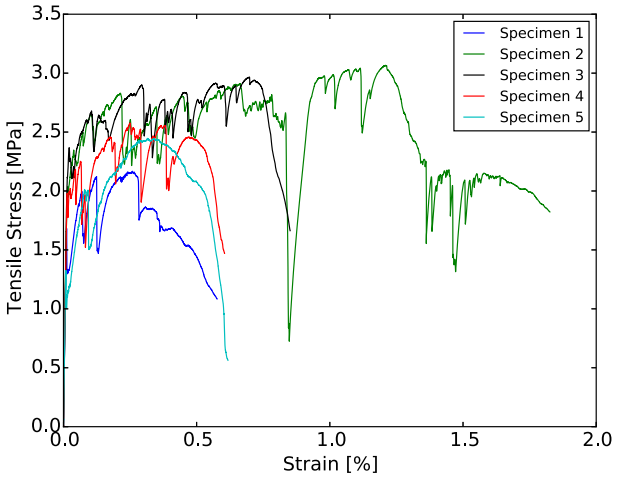


**Fig. 20.** Tensile performance of X series.

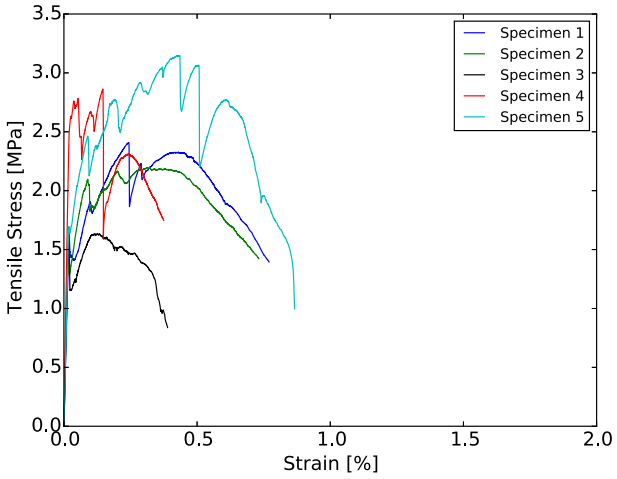


**Fig. 21.** Tensile performance of Y series.

whereas others (Roussel [67]) have proposed a rheology based failure criterion. As the print material develops from a highly viscous to a solid state after deposition, both approaches have merit. An extensive discussion of this issue falls outside the scope of this study. For now, a rheology based approximation of the expected buildability was calculated to be 17 layers, based on the measured bulk yield stress of $(34.26 \pm 1.98)$ kPa, an assumed mass density of 2000 kg/m$^3$, and an average layer height of 0.01 m. The mixture has an excessive open time of more than 12 h. Therefore, structural build-up during printing was ignored in this estimation. The progress of the object printing experiment is shown in Fig. 17. The object collapsed during printing of the 14*th* layer. The calculated 17 layers apparently is a considerable overestimation, but it is nevertheless in the same order of magnitude. The deviation is likely due to stability effects that depend on the 3D geometry, density variations, and dynamically changing loads caused by the deposition of the print filament. It may nevertheless be concluded that the mixture is printable, and further adaptations of it should be considered to improve buildability.

### 4.3. Mechanical properties

Among all evaluated mixtures, only those reinforced by 2 vol.% of fibres were evaluated mechanically. The influence of 0.3 and 0.4% by solid weight of VA, as well as the maximum grain size of the sand, were evaluated through compressive strength and four-point bending tests.

All tested mixtures delivered flexural hardening and developed a ductile behaviour, as given in Fig. 18. Nevertheless, multiple cracks were more often observed in X series and in mixtures in which the smaller grain size of the sand was employed. This behaviour was expected since the size of aggregates influences the number of cracks and the crack pattern, as demonstrated by [68]. Additionally,

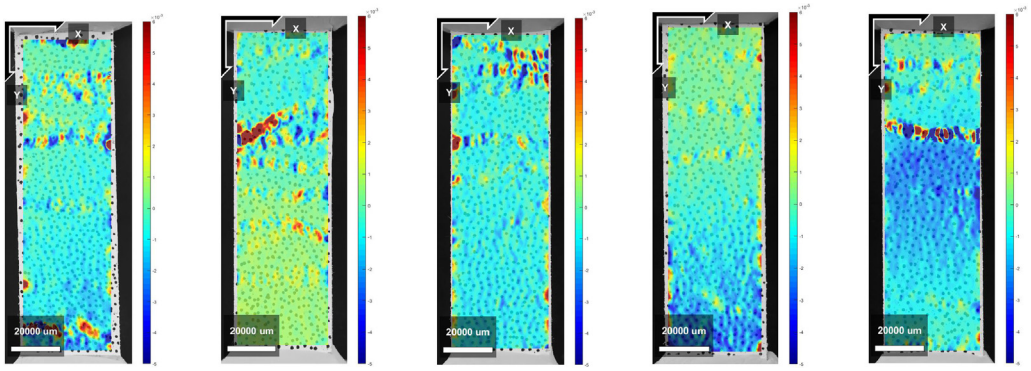


(a) Specimen 1 (b) Specimen 2 (c) Specimen 3 (d) Specimen 4 (e) Specimen 5

**Fig. 22.** Crack pattern obtained from DIC analysis on X samples - Horizontal Deformations.

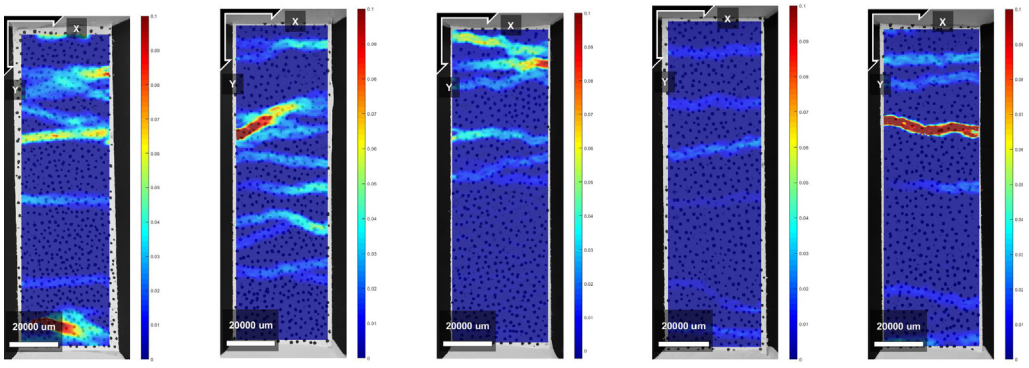


(a) Specimen 1 (b) Specimen 2 (c) Specimen 3 (d) Specimen 4 (e) Specimen 5

**Fig. 23.** Crack pattern obtained from DIC analysis on X samples - Vertical Deformations.

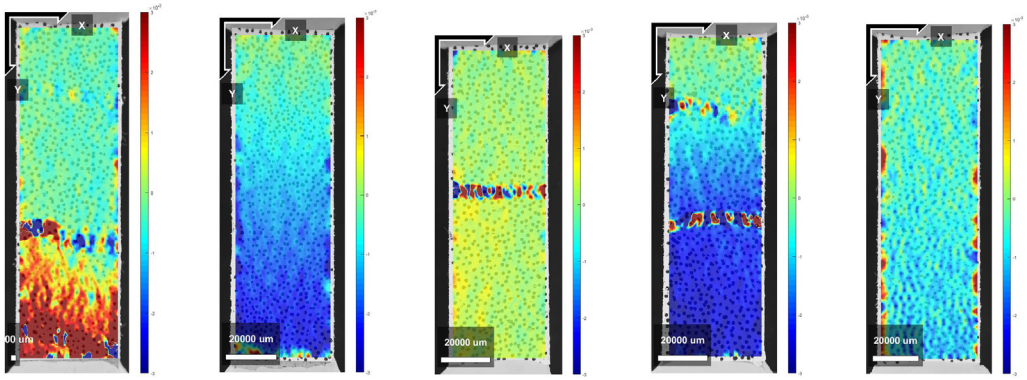


(a) Specimen1 (b) Specimen 2 (c) Specimen 3 (d) Specimen 4 (e) Specimen 5

**Fig. 24.** Crack pattern obtained from DIC analysis on Y samples - Horizontal Deformations.

larger aggregates can also make the dispersion of fibres more difficult, decreasing the number of fibres effectively bridging the cracks [69]. Fig. 19 summarizes the results from the four-point bending test.

Meanwhile, the compressive strength values of all analysed mixtures, listed in Table 6, were significantly higher for X's, in comparison with the Y's. The amount of VA employed in the composites did not significantly influence the compressive strength or the flexural behaviour of the analysed composites, with the exception of the ones with sand up to 0.5 mm. Only in this case, composites with 0.4 wt.% of VA delivered higher performance. As demonstrated, the mechanical performance was not influenced by the amount of VA employed on X mixtures and 0.4 wt.% improves Y-S05 series.

Moreover, as discussed in the previous section, only XVA3PVA20 and YVA4PVA20-S05 were suitable for printing. Therefore, only these two mixtures were chosen to be investigated employing an uni-axial tensile test, in order to confirm their strain hardening and multiple crack behaviour. In Figs. 20 and 21 the "tensile stress versus strain" curve of both mixtures are plotted. It could be confirmed that the modified composites mix-design also showed high ductility and strain hardening behaviour.

In Figs. 22, 23, 24, 25 the last pictures from the DIC analyses are shown. In pictures depicting the vertical displacements only elongations were shown. Regions in blue suffered less deformation than regions with colours closer to red, where the cracks are. On pictures showing the horizontal displacements elongations and compressions are shown. There, zero displacements were demonstrated with yellow colours with elongations been demonstrated in red and compressions in blue. Through the DIC analysis the horizontal displacements could also be captured. Where the cracks were concentrated it was possible to observe areas with compressive values and some others in tension. These regions are believed to have fibres oriented with different angles, which emphasizes the importance of fibre dispersion in this type of composite. It is possible to observe that all samples developed at least two cracks, and specimens from the X series resulted in higher tensile performances and considerably greater number of cracks.

## 5. Conclusions

Through the experimental procedure carried out in this study, a methodology was presented to develop printable cementitious composite mix-designs based on fundamental rheological properties. The influence of rheology modifiers on the fresh and hardened state was evaluated for application in high performance cementitious composites. Visual inspection together with rheology parameters evaluation were employed to obtain an optimized SHCC mixture in terms of

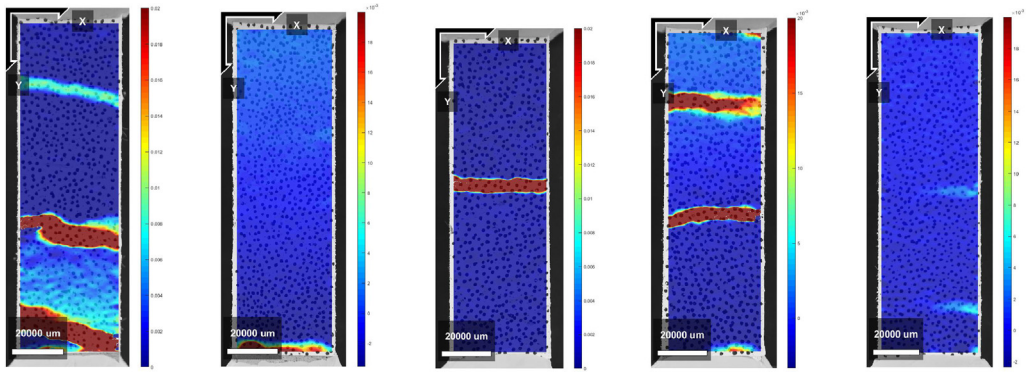


(a) Specimen 1 (b) Specimen 2 (c) Specimen 3 (d) Specimen 4 (e) Specimen 5

**Fig. 25.** Crack pattern obtained from DIC analysis on Y samples - Vertical Deformations.

printability, shape stability and strain hardening behaviour. Printing experiments were conducted to compare the pumpability and extrudability of various mixtures. One mixture was used to print an object and evaluate buildability. Mechanical tests were performed to confirm the strain hardening behaviour of the developed mixtures. In summary the following conclusions can be drawn:

- Ram extruder with the Benbow-Bridgwater model are appropriate tools to develop printable cementitious composites. However, it is important to notice that the method has limitations. One example was the inability to predict the blockage of some mixtures in the pump.
- The employment of rheology modifiers is crucial for the development of high ductility cementitious composites, with dough-like consistency in the fresh state.
- The liquid-to-solid ratio of the solid suspension is more relevant to the shape stability of printable mixtures, than the amount of superplasticizer.
- For the development of printable cementitious mixtures, the particle size distribution and the liquid-to-total surface area of all solids are more relevant than the employment of rheology modifiers.
- The amount of rheology modifiers employed in the mix did not significantly influence the mechanical properties of most evaluated composites.
- XVA3PVA20 and YVA4PVA20-S05 are composites which have proven to have high mechanical performance and superior printing quality and therefore, must be considered for further developments in the construction printing industry.

## CRediT authorship contribution statement

**Stefan Chaves Figueiredo:** Conceptualization, Methodology, Software, Validation, Formal analysis, Investigation, Data curation, Writing - original draft, Writing - review & editing. **Claudia Romero Rodríguez:** Conceptualization, Methodology, Validation, Investigation, Writing - original draft, Writing - review & editing. **Zeeshan Y. Ahmed:** Validation, Investigation, Resources. **D.H. Bos:** Investigation. **Yading Xu:** Validation, Investigation, Writing - review & editing. **Theo M. Salet:** Resources, Supervision. **Oğuzhan Çopuroğlu:** Resources, Writing - review & editing, Supervision. **Erik Schlangen:** Resources, Writing - review & editing, Supervision. **Freek P. Bos:** Investigation, Resources, Writing - original draft, Writing - review & editing, Supervision.

## Acknowledgements

This study was performed as part of the 2017 4.TU Lighthouse project '3D Concrete Printing for Structural Applications', that was performed jointly by the Eindhoven and Delft Universities of Technology. The support of the 4TU.Federation is gratefully acknowledged

In addition, the first author would like to acknowledge the funding from Science Without Borders from the National Council for Scientific and Technological Development of Brazil (201620/2014-6). The second author acknowledges the financial support from the Construction Technology Research Program funded by the Ministry of Land, Infrastructure and Transport of the Korean Government under the grant 17SCIP-B103706-03. The fifth author acknowledges the financial support from China Scholarship Council (CSC) under the grant CSC No. 201708110187.

The concrete printing was performed at the Eindhoven University of Technology (TU/e) 3D Concrete Printing (3DCP) Facility. The TU/e research program on 3DCP is co-funded by a partner group of enterprises and associations, that on the date of writing consisted of (alphabetical order) Ballast Nedam, BAM Infraconsult bv, Bekaert, Concrete Valley, CRH, Cybe, Saint-Gobain Weber Beamix, SGS Intron, SKKB, Van Wijnen, Verhoeven Timmerfabriek, and Witteveen+Bos. Their support is gratefully acknowledged.

Finally, the authors acknowledge the support of Kuraray by providing the PVA fibres used in this study.

## Data availability

The raw/processed data required to reproduce these findings cannot be shared at this time as the data also forms part of an ongoing study.

## References

[1] B.E. Allmon, C.T. Haas, J.D. Borcherding, P.M. Goodrum, U.S. construction labor productivity trends, 1970–1998, Journal of construction engineering and management 126 (April) (2000) 97–104.
[2] R.R. Ramrez, L.F.C. Alarcón, P. Knights, Benchmarking system for evaluating management practices in the construction industry, Journal of Management in Engineering 20 (3) (2004) 110–117.
[3] H. Kodama, Automatic method for fabricating a three-dimensional plastic model with photo-hardening polymer, Review of Scientific Instruments 52 (11) (1981) 1770–1773.
[4] E. Sachs, M. Cima, J. Cornie, D. Brancazio, J. Bredt, A. Curodeau, T. Fan, S. Khanuja, A. Lauder, J. Lee, S. Michaels, Three-dimensional printing: the physics and implications of additive manufacturing, CIRP Annals - Manufacturing Technology 42 (1) (1993) 257–260.
[5] A.C. De Leon, Q. Chen, N.B. Palaganas, J.O. Palaganas, J. Manapat, R.C. Advincula, High performance polymer nanocomposites for additive manufacturing applications, Reactive and Functional Polymers 103 (2016) 141–155.
[6] L.E. Murr, S.M. Gaytan, F. Medina, E. Martinez, J.L. Martinez, D.H. Hernandez, B.I. Machado, D.A. Ramirez, R.B. Wicker, Characterization of Ti-6Al-4V open cellular foams fabricated by additive manufacturing using electron beam melting, Materials Science and Engineering A 527 (7-8) (2010) 1861–1868.
[7] J. Luo, H. Pan, E.C. Kinzel, Additive manufacturing of glass, Journal of Manufacturing Science and Engineering 136 (6) (2014) 061024.
[8] J. Willmann, M. Knauss, T. Bonwetsch, A.A. Apolinarska, F. Gramazio, M. Kohler, Robotic timber construction - expanding additive fabrication to new dimensions, Automation in Construction 61 (2016) 16–23.
[9] D. Herzog, V. Seyda, E. Wycisk, C. Emmelmann, Additive manufacturing of metals, Acta Materialia 117 (2016) 371–392.
[10] D-Shape, What is D-Shape.
[11] B. Khoshnevis, Automated construction by contour crafting - related robotics and information technologies, Automation in Construction 13 (1) (2004) 5–19.
[12] S. Lim, R.A. Buswell, T.T. Le, S.A. Austin, A.G. Gibb, T. Thorpe, Developments in construction-scale additive manufacturing processes, Automation in Construction 21 (1) (2012) 262–268.
[13] C. Gosselin, R. Duballet, P. Roux, N. Gaudillière, J. Dirrenberger, P. Morel, Large-scale 3D printing of ultra-high performance concrete - a new processing route for architects and builders, Materials and Design 100 (2016) 102–109.
[14] E. Lloret Fritschi, L. Reiter, T. Wangler, F. Gramazio, M. Kohler, R.J. Flatt, Smart dynamic casting slipforming with flexible formwork - inline measurement and control, HPC/CIC Tromsø 2017. Eleventh High Performance Concrete (11th HPC) and the Second Concrete Innovation Conference (2nd CIC), Norwegian Concrete Association, Tromsø, 2017,
[15] N. Hack, W.V. Lauer, Mesh-mould: robotically fabricated spatial meshes as reinforced concrete formwork, Architectural Design 84 (3) (2014) 44–53.
[16] F. Bos, R. Wolfs, Z. Ahmed, T. Salet, Additive manufacturing of concrete in construction: potentials and challenges of 3D concrete printing, Virtual and Physical Prototyping 11 (3) (2016) 209–225.
[17] Y.W.D. Tay, B. Panda, S.C. Paul, N.A.N. Mohamed, M.J. Tan, K.F. Leong, 3D printing trends in building and construction industry: a review, Virtual and Physical Prototyping 12 (3) (2017) 261–276.
[18] D. Delgado, P. Clayton, W.J.O. Brien, C. Seepersad, M. Juenger, R. Ferron, S. Salamone, Applications of additive manufacturing in the construction industry – a forward-looking review, Automation in Construction 89 (August 2017) (2018) 110–119.
[19] H.A. Jassmi, F.A. Najjar, A.-h. I. Mourad, Large-scale 3D printing : the way forward large-scale 3D printing: the way forward, IOP Conf. Series: Materials Science and Engineering, IOP Publishing. 2018, pp. 324.
[20] B. Nematollahi, M. Xia, J. Sanjayan, Current progress of 3D concrete printing technologies, 34th International Symposium on Automation and Robotics in Construction (ISARC 2017), Taipei, Taiwan, 2017,
[21] S. Hamidreza, J. Corker, M. Fan, Additive manufacturing technology and its implementation in construction as an eco-innovative solution, Automation in Construction 93 (May) (2018) 1–11.

[22] R.A. Buswell, W.R.L.D. Silva, S.Z. Jones, J. Dirrenberger, Cement and concrete research 3D printing using concrete extrusion: a roadmap for research, Cement and Concrete Research 112 (May) (2018) 37–49.
[23] M.A. Guowei, W. Li, J.U. Yang, State-of-the-art of 3D printing technology of cementitious material – an emerging technique for construction, Science China Technological Sciences 61 (4) (2018) 475–495.
[24] Agence France-Presse, World's First 3D-Printed Bridge Opens to Cyclists in Netherlands, 2017.
[25] K. Subrin, T. Bressac, S. Garnier, A. Ambiehl, E. Paquet, B. Furet, Improvement of the mobile robot location dedicated for habitable house construction by 3D printing, IFAC-PapersOnLine 51 (11) (2018) 716–721. 16th IFAC Symposium on Information Control Problems in Manufacturing INCOM 2018.
[26] A. Kazemian, X. Yuan, E. Cochran, B. Khoshnevis, Cementitious materials for construction-scale 3D printing: laboratory testing of fresh printing mixture, Construction and Building Materials 145 (2017) 639–647.
[27] R.A. Buswell, R.C. Soar, A.G.F. Gibb, A. Thorpe, Freeform construction: mega-scale rapid manufacturing for construction, Automation in Construction 16 (2) (2007) 224–231.
[28] P. Wu, J. Wang, X. Wang, A critical review of the use of 3-D printing in the construction industry, Automation in Construction 68 (2016) 21–31.
[29] G.D. Schutter, K. Lesage, V. Mechtcherine, V. Naidu, G. Habert, I. Agusti-juan, Cement and concrete research vision of 3D printing with concrete – technical, economic and environmental potentials, Cement and Concrete Research 112 (August) (2018) 25–36.
[30] V. Nerella, V.N. Krause, M. Näther, M. Mechtcherine, 3D printing technology for on-site construction, Concr. Plant. Int. (2016) 36–41.
[31] V.N. Schach, R. Krause, M. Näther, M. Nerella, CONPrint3D: 3D concrete-printing as an alternative for masonry, Bauingenieur 9 (2017) 355–363.
[32] F.P. Bos, Z.Y. Ahmed, E.R. Jutinov, T.A. Salet, Experimental exploration of metal cable as reinforcement in 3D printed concrete, Materials 10 (11). (2017)
[33] D. Asprone, F. Auricchio, C. Menna, V. Mercuri, 3D printing of reinforced concrete elements: technology and design approach, Construction and Building Materials 165 (2018) 218–231.
[34] R. Duballet, O. Baverel, J. Dirrenberger, Space truss masonry walls with robotic mortar extrusion, Structures (November) (2018) 1–7.
[35] B. Panda, S. Chandra Paul, M. Jen Tan, Anisotropic mechanical performance of 3D printed fiber reinforced sustainable construction material, Materials Letters 209 (2017) 146–149.
[36] Y. Weng, M. Li, Z. Liu, W. Lao, B. Lu, D. Zhang, M.J. Tan, Printability and fire performance of a developed 3D printable fibre reinforced cementitious composites under elevated temperatures, Virtual and Physical Prototyping 0 (0) (2018) 1–9.
[37] F.P. Bos, E. Bosco, T.A.M. Salet, Ductility of 3D printed concrete reinforced with short straight steel fibers, Virtual and Physical Prototyping 14 (2) (2019) 160–174.
[38] V.C. Li, On engineered cementitious composites (ECC). A review of the material and its applications, Journal of Advanced Concrete Technology 1 (3) (2003) 215–230.
[39] S. Müller, V. Mechtcherine, Fatigue behaviour of strain-hardening cement-based composites (SHCC), Cement and Concrete Research 92 (2017) 75–83.
[40] V.C. Li, H. Horii, P. Kabele, T. Kanda, Y. Lim, Repair and retrofit with engineered cementitious composites, Engineering Fracture Mechanics 65 (2-3) (2000) 317–334.
[41] F. Altmann, V. Mechtcherine, Durability design strategies for new cementitious materials, Cement and Concrete Research 54 (2013) 114–125.
[42] D.G. Soltan, V.C. Li, A self-reinforced cementitious composite for building-scale 3D printing, Cement and Concrete Composites 90 (2018) 1–13.
[43] V.N. Nerella, H. Ogura, V. Mechtcherine, Incorporating reinforcement into digital concrete construction, Proceedings of the IASS Symposium 2018 Creativity in Structural Design, Boston, 2018,
[44] M. Rubio, M. Sonebi, S. Amziane, 3D Printing of fibre cement-based materials: fresh and rheological performances, in: S. AMZIANE, M. SONEBI (Eds.), 2nd International Conference On Bio-Based Building Materials, RILEM, 119 (PRO 119), Clermont Ferrand, 2017,
[45] G. Ma, Z. Li, L. Wang, Printable properties of cementitious material containing copper tailings for extrusion based 3D printing, Construction and Building Materials 162 (2018) 613–627.
[46] R.J. Wolfs, F.P. Bos, T.A. Salet, Early age mechanical behaviour of 3D printed concrete: numerical modelling and experimental testing, Cement and Concrete Research 106 (February) (2018) 103–116.
[47] M. Hambach, D. Volkmer, Properties of 3D-printed fiber-reinforced Portland cement paste, Cement and Concrete Composites 79 (2017) 62–70.
[48] X. Zhou, Z. Li, Characterization of rheology of fresh fiber reinforced cementitious composites through ram extrusion, Materials and Structures 38 (February) (2005) 17–24.
[49] J.J. Benbow, The dependence of output rate on die shape during catalyst extrusion, Chemical Engineering Science 26 (1971) 1467–1473.
[50] J.J. Benbow, J. Bridgwater, The influence of formulation on extrudate structure and strength, Chemical Engineering Science 42 (1987) 753–766.
[51] J.J. Benbow, E.W. Oxley, The extrusion mechanics of pastes- the influence of paste formulation extrusion parameters, Chemical Engineering Science 42 (1967) (1987) 1467–1473.
[52] S. Srinivasan, D. Deford, P. Shah, The use of extrusion rheometry in the development of extrudate fibre-reinforced cement composites, Concrete Science and Engineering 1 (11) (1999) 26–36.
[53] R. Nath Das, C.D. Madhusoodana, K. Okada, Rheological studies on cordierite honeycomb extrusion, Journal of the European Ceramic Society 22 (16) (2002) 2893–2900.
[54] X. Zhou, Z. Li, M. Fan, H. Chen, Cement & concrete composites rheology of semi-solid fresh cement pastes and mortars in orifice extrusion, Cement and Concrete Composites 37 (2013) 304–311.
[55] R. Teixeira, G. Tonoli, S. Santos, J. Fiorelli, H. Savastano, Jr, F.R. Lahr, Extruded cement based composites reinforced with sugar cane bagasse fibres, Key Engineering Materials 517 (2012) 450–457.
[56] S.F. Santos, R. Schmidt, A.E.F.S. Almeida, G.H.D. Tonoli, H. Savastano, Supercritical carbonation treatment on extruded fibre – cement reinforced with vegetable fibres, Cement & Concrete Composites 56 (2015) 84–94.
[57] V. da Costa Correia, S.F. Santos, R. Soares Teixeira, H. Savastano Junior, Nanofibrillated cellulose and cellulosic pulp for reinforcement of the extruded cement based materials, Construction and Building Materials 160 (2018) 376–384.
[58] S.F.U. Ahmed, H. Mihashi, A review on durability properties of strain hardening fibre reinforced cementitious composites (SHFRCC), Cement and Concrete Composites 29 (5) (2007) 365–376.
[59] M. Åđahmaran, V.C. Li, Durability properties of micro-cracked ECC containing high volumes fly ash, Cement and Concrete Research 39 (11) (2009) 1033–1043.
[60] J. Zheng, W.B. Cadson, J.S. Reed, Flow mechanics on extrusion through a square-entry die, Journal of the American Ceramic Society (75) (1992) 3011–3016.
[61] J.J. Benbow, S.H. Jazayeri, J. Bridgwater, The flow of pastes through dies of complicated geometry, Powder Technology 65 (1991) 393–401.
[62] J. Zhou, S. Qian, M.G. Sierra Beltran, G. Ye, K. Breugel, V.C. Li, Development of engineered cementitious composites with limestone powder and blast furnace slag, Materials and Structures 43 (6) (2010) 803–814.
[63] P. Wang, F.H. Wittmann, P. Zhang, E. Lehmann, T. Zhao, Durability and service life of elements made with SHCC under imposed strain, SHCC3 - 3rd International RILEM Conference on Strain Hardening Cementitious Composites, 2014, pp. 33–41.
[64] Y.J.M. Soto, Adequação de formulações para a produção de placas de fibrocimento por extrusão,Ph.D. thesis. Escola Politécnica da Universidade de São Paulo. 2010.
[65] R. Wolfs, F. Bos, T. Salet, Early age mechanical behaviour of 3D printed concrete: numerical modelling and experimental testing, Cement and Concrete Research 106 (2018) 103–116.
[66] J. Blaber, B. Adair, A. Antoniou, Ncorr: open-source 2D digital image correlation Matlab software, Experimental Mechanics 55 (6) (2015) 1105–1122.
[67] N. Roussel, Rheological requirements for printable concretes, Cement and Concrete Research (April) (2018) 1–10.
[68] X. Huang, R. Ranade, W. Ni, V.C. Li, Development of green engineered cementitious composites using iron ore tailings as aggregates, Construction and Building Materials 44 (2013) 757–764.
[69] G. Song, G.V. Zijl, Tailoring ECC for commercial application, Proceedings of the 6th RILEM symposium on fiber (September) (2004) 1391–1400.